Developmental Biology 441 (2018) 146–158

Contents lists available at ScienceDirect

Developmental Biology

journal homepage: www.elsevier.com/locate/developmentalbiology

Characterization of C-C motif chemokine ligand 4 in the porcine endometrium during the presence of the maternal–fetal interface

Whasun Lim[a,1], Hyocheol Bae[b,1], Fuller W. Bazer[c], Gwonhwa Song[b,*]

[a] Department of Biomedical Sciences, Catholic Kwandong University, Gangneung 25601, Republic of Korea
[b] Institute of Animal Molecular Biotechnology and Department of Biotechnology, College of Life Sciences and Biotechnology, Korea University, Seoul 02841, Republic of Korea
[c] Center for Animal Biotechnology and Genomics and Department of Animal Science, Texas A&M University, College Station 77843, TX, USA

ARTICLE INFO

Keywords:
CCL4
CCR5
Endometrium
Proliferation
Pregnancy

ABSTRACT

Chemokines and their receptors play a crucial role in embryo implantation at the maternal–fetal interface during pregnancy. In this study, we investigated the role of CCL4 in development of the porcine endometrium in the early gestational period. Porcine CCL4 showed high similarity with the human counterpart, and mRNA expression of *CCL4* and its receptor (*CCR5*) was predominantly present in the endometrium during early pregnancy. Treatment with CCL4 increased proliferation of porcine uterine luminal epithelial (pLE) cells by activation of PI3K and MAPK signal transduction. In addition, CCL4 recovered the endoplasmic-reticulum stress–reduced proliferation and decreased the unfolded protein response in pLE cells. Besides, the lipopolysaccharide-activated NF-κB pathway was suppressed in response to CCL4 in pLE cells. Inhibition of CCR5 decreased the proliferation of pLE cells and activation of the PI3K and MAPK pathways by CCL4. Furthermore, CCL4 enhanced conceptus-maternal interactions between porcine trophectoderm (pTr) cells and pLE cells during early pregnancy by activating expression of migration and implantation-related genes. Collectively, the results suggest that CCL4 may improve successful implantation in early pregnancy in pigs.

1. Introduction

For improvement of the implantation rate to increase livestock production, it is important to understand reciprocal mechanisms at the maternal–fetal interface during early pregnancy (Bazer et al., 2009; Mathew et al., 2016). Cellular differentiation and migration of the conceptus for successful implantation depend on secretion of the endometrial histotroph in mammals during pregnancy (Spencer and Bazer, 2004). For production and transfer of histotrophic nutrition, hormones, and cytokines from the endometrium to the conceptus, the development of endometrial glands by hyperplasia and hypertrophy is required. Furthermore, deficiency of the endometrial secretion reduces placentation and the survival and growth of the conceptus (Cha and Dey, 2014). To investigate orchestration of the conceptus–endometrium interaction, the pig is a good animal model owing to prolonged peri-implantation and implantation periods and epitheliochorial placentation with availability of a separated conceptus and maternal endometrial tissues. Although some studies have identified the genes crucial for development of the conceptus and uterus in the early gestational period in pigs (Chen et al., 2015; Tayade et al., 2006), elucidation of mechanistic signal transduction in both tissues is necessary to better understand the reciprocal interaction.

Chemokines are small chemotactic cytokines classified into four subfamilies (CXC, CC, CX3C, and C) (Zlotnik and Yoshie, 2012). Chemokines regulate a variety of biological functions such as angiogenesis, carcinogenesis, metastasis, embryogenesis, transplantation, and initiation of an immune response to an infection (Borroni et al., 2008; Zlotnik and Yoshie, 2012). Specifically, chemokines and their receptors play an important role in the communication between the conceptus and mother and thus allow an allogeneic embryo and placenta to coexist at the maternal–fetal interface (Du et al., 2014; Red-Horse et al., 2001). Among the relevant chemokines, CCL4 is strongly expressed in the secretory-phase endometrium in response to a high progesterone concentration, and expression of CCL4 correlates with the number of endometrial natural killer (NK) cells as a potential chemoattractant for NK cells (Kitaya et al., 2003). In addition, CCL4 commonly binds to both CCR1 and CCR5 for recruitment of monocytes, eosinophils, basophils, and lymphocytes (Di Marzio et al., 2005). In a previous study, we demonstrated increased expression of CCR1 in the glandular epithelium (GE) and luminal epithelium (LE) of the

* Correspondence to: Department of Biotechnology, College of Life Sciences and Biotechnology, Korea University, Seoul 02841, Republic of Korea.
E-mail address: ghsong@korea.ac.kr (G. Song).
[1] These authors contributed equally to this work.

https://doi.org/10.1016/j.ydbio.2018.06.022
Received 26 February 2018; Received in revised form 27 June 2018; Accepted 29 June 2018
Available online 02 July 2018
0012-1606/

porcine endometrium in the early gestational period (Jeong et al., 2017). Although the expression of CCL4 has been identified in the endometrium and trophoblast during early pregnancy in pigs (Wessels et al., 2011), little is known about its function at the maternal–fetal interface.

Therefore, the specific aims of the present study were 1) to analyze the cell-specific expression of *CCL4* and another receptor gene *CCR5* in the porcine endometrium during the estrus cycle and pregnancy, 2) to investigate the effects of CCL4 on proliferation and cell cycle phases of porcine uterine luminal epithelial (pLE) cells, 3) to determine intracellular signaling pathways regulated by CCL4 and CCR5 in pLE cells, 4) to estimate inhibitory effects of CCL4 on endoplasmic reticulum (ER) stress and inflammation signs in pLE cells, and 5) to investigate conceptus-maternal interactions using pTr and pLE cells. Our results suggest that CCL4 and its receptors improve implantation through an increase in porcine endometrial receptivity at the maternal–fetal interface in the early gestational period.

2. Material and methods

2.1. Sequence analysis

For pairwise comparisons and multiple sequence alignment, the amino acid sequences of *CCL4* genes from various species were aligned in the Geneious Pro software, version 10.2.2 (Biomatters Ltd.) (Kearse et al., 2012), with default penalties for gaps, and the protein weight matrix of Blocks Substitution Matrix (BLOSUM; Biomatters, Ltd.). A phylogenetic tree was constructed by the neighbor-joining method (Gascuel and Steel, 2006) in Geneious Pro, version 10.2.2. To determine the confidence level for each internal node in the phylogenetic tree, 1000 nonparametric bootstrap replications were executed (Felsenstein, 1985).

2.2. Experimental animals and animal care

Sexually mature gilts of similar age, weight, and genetic background were observed daily for estrus (day 0) and went through at least two estrous cycles of normal duration (18–21 days) before enrollment in the experiments. All experimental and surgical procedures were compliant with the Guide for Care and Use of Agricultural Animals in Teaching and Research and were approved by the Institutional Animal Care and Use Committee of Texas A & M University.

2.3. Experimental design and tissue collection

Gilts were assigned randomly to either cyclic status (day 9, 12, or 15 of the estrous cycle) or pregnant status (day 9, 10, 12, 13, 14, 15, 20, or 30 of pregnancy). Those in the pregnant group were mated when found to be in estrus, and 12 or 24 h later, the gilts were ovariohysterectomized on day 9, 12, or 15 of the estrous cycle or on day 9, 10, 12, 13, 14, 15, 20, or 30 of pregnancy (n = 3–4 pigs per day per status). For confirmation of pregnancy prior to implantation, the lumen of each uterine horn was flushed with 20 mL of physiological saline and examined for the presence of morphologically normal conceptuses. Uteri from cyclic and pregnant gilts were processed to obtain several slices (~ 0.5 cm) of the entire uterine wall in the middle of each uterine horn. The tissue was fixed in fresh 4% paraformaldehyde in phosphate-buffered saline (PBS; pH 7.2), and then embedded in Paraplast-Plus (Leica Microsystems, Wetzlar, Germany).

2.4. Cell culture

An immortalized pLE cell line was originally established by Wang and colleagues by stable transfection of primary pLE cells with a replication-defective retroviral (SV40) vector (Wang et al., 2000). That cell line was obtained and used in this *in vitro* study. pLE cells have typical epithelium like cobblestone-shaped morphology and yield positive staining with antibodies against epithelium-specific cytokeratin and negative staining for vimentin (Wang et al., 2000). pLE cells form a single monolayer at confluence. All analyses in this study were performed on pLE cells between passages 25 and 30. Briefly, monolayer cultures of pLE cells were grown to 80% confluence in Dulbecco's modified Eagle's medium (DMEM)/F12 1:1 culture medium containing 20% fetal bovine serum (FBS) in 100 mm tissue culture dishes. The porcine trophectoderm (pTr) cell line, established using trophectoderm cells from Day 12 pregnant gilts, were cultured and used in the present *in vitro* studies as described previously (Jaeger et al., 2005). Monolayer cultures of pTr cells were grown in DMEM/F12 1:1 medium containing 10% FBS. For assays, *in vitro*–cultured pLE and pTr cells were serum-starved for 24 h and then subjected to various treatments.

2.5. RNA isolation

Total cellular RNA was isolated from the endometrium of the cyclic and pregnant gilts by means of the TRIzol Reagent (Invitrogen, Carlsbad, CA, USA), and purified with the RNeasy Mini Kit (Qiagen, Hilden, Germany). The quantity and quality of total RNA were determined by spectrophotometry and denaturing agarose gel electrophoresis, respectively.

2.6. Quantitative polymerase chain reaction (PCR) analysis

Specific primers were designed using sequences from the GenBank database in Primer 3 (ver. 4.0.0) as illustrated in Supplemental Table 1. All primers were synthesized by Bioneer (Daejeon, Republic of Korea). Gene expression levels were measured using SYBR Green (Sigma, St. Louis, MO, USA) on a StepOnePlus Real-Time PCR System (Applied Biosystems, Waltham, MA, USA). The cycling conditions were 95 °C for 3 min, followed by 40 cycles at 95 °C for 20 s, 64 °C for 40 s, and 72 °C for 1 min with a melting curve program (increasing the temperature from 55 to 95 °C at 0.5 °C per 10 s) and continuous fluorescence measurements. Sequence-specific products were identified by generating a melting curve in which the C_T value represented the number of cycles required for the fluorescent signal to exceed the background level. Relative gene expression was quantified by the $2^{-\Delta\Delta CT}$ method. The glyceraldehyde 3-phosphate dehydrogenase (*GAPDH*) gene served as an endogenous control to standardize the amount of RNA in each reaction.

2.7. Cloning of partial cDNA for porcine CCL4 and CCR5

cDNA was synthesized using the AccuPower RT PreMix (Bioneer Inc.). Partial cDNAs for porcine *CCL4* and *CCR5* mRNAs were amplified with specific primers based on data for porcine *CCL4* (GenBank accession No. NM_213779.1; forward: 5′- GAA GCT CTG CGT GAC TGT CC-3′, reverse: 5′-CAG TCA TCA CTG GGG TTG G-3′) and porcine *CCR5* (GenBank accession No. NP_001001618.1; forward: 5′- GCT GTT CCT CTT CAC CAT CC-3′, reverse: 5′- TGA GGG CTG CAT GTA TAA CG-3′). Partial cDNAs for *CCL4* and *CCR5* were gel-extracted and cloned into the TOPO TA cloning vector (Invitrogen).

2.8. In situ hybridization analysis

After verification of the sequences, the plasmids containing gene sequences were amplified with T7- and SP6-specific primers (T7: 5′-TGT AAT ACG ACT CAC TAT AGG G-3′; SP6: 5′-CTA TTT AGG TGA CAC TAT AGA AT-3′), and then digoxigenin (DIG)-labeled RNA probes were transcribed by means of the DIG RNA labeling kit (Roche, Indianapolis, IN, USA). The tissue slices were deparaffinized, rehydrated, treated with 1% Triton X-100 in PBS for 20 min, and then washed twice in diethyl pyrocarbonate (DEPC)-treated PBS. After postfixation in 4% paraformaldehyde, the tissue slices were incubated

in a prehybridization mixture containing 50% of formamide and incubated in 4 standard saline citrate buffer for at least 10 min at room temperature. After hybridization and blocking steps, the slices were incubated overnight with a sheep anti-DIG antibody conjugated to alkaline phosphatase (Roche). The signal was visualized by exposure to a solution containing 0.4 mM 5-bromo-4-chloro-3-indolyl phosphate, 0.4 mM nitroblue tetrazolium, and 2 mM levamisole (Sigma-Aldrich).

2.9. Reagents

Recombinant human CCL4 (catalog number: 271-BME/CF) was purchased from R & D Systems (Minneapolis, MN, USA). Because there is no commercially available recombinant porcine CCL4, recombinant human CCL4 was used in this study. Tunicamycin (catalog number: T7765), LPS (catalog number: L4391) and Maraviroc (catalog number: PZ0002) were purchased from Sigma Chemical Co. Antibodies against human phosphorylated (p)-AKT (Ser^{473}, catalog number: 4060), human p-ERK1/2 (Thr^{202}/Tyr^{204}, catalog number: 9101), human p-JNK (Thr^{183}/Tyr^{185}, catalog number: 4668), human p-P38 (Thr^{180}/Tyr^{182}, catalog number: 4511), human p-p70S6K (Thr^{421}/Ser^{424}, catalog number: 9204), human p-S6 ($Ser^{235/236}$, catalog number: 2211), human p-cyclin D1 (Thr^{286}, catalog number: 3300), human p-eIF2α (Ser^{51}, catalog number: 3398), human p-NF-κB (Ser^{536}, catalog number: 3033), human p-IKKαβ ($Ser^{176/180}$, catalog number: 2697), human p-IRAK (Thr^{345}/Ser^{346}, catalog number: 11927), mouse p-TAK1 (Ser^{412}, catalog number: 9339), mouse AKT (catalog number: 9272), rat ERK1 and −2 (catalog number: 4695), human JNK (catalog number: 9252), human P38 (catalog number: 9212), human p70S6K (catalog number: 9202), human S6 (catalog number: 2217), human cyclin D1 (catalog number: 2922), human eIF2α (catalog number: 5324), human IRE1α (catalog number: 3294), human NF-κB (catalog number: 8242), human IKKα (catalog number: 11930), human IKKβ (catalog number: 2678), human IRAK (catalog number: 4363), human TAK1 (catalog number: 5206), and against human MyD88 (catalog number: 4283) were acquired from Cell Signaling Technology (Beverly, MA, USA). Antibodies against human p-PERK (Thr^{981}, catalog number: sc-32577), human PERK (catalog number: sc-13073), human ATF6α (catalog number: sc-166659), human GRP78 (catalog number: sc-13968), and against mouse GADD153 (catalog number: sc-7351) were purchased from Santa Cruz Biotechnology (Dallas, TX, USA). Inhibitors of ERK1 and -2 (U0126, catalog number: EI282), JNK (SP600125, catalog number: EI305), and P38 (SB203580, catalog number: EI286) were acquired from Enzo Life Sciences (Farmingdale, NY, USA), and a PI3K/AKT inhibitor (Wortmannin, catalog number: 9951) from Cell Signaling Technology.

2.10. Proliferation assays

These assays were conducted using the Cell Proliferation ELISA Kit, BrdU (cat. No. 11647229001, Roche). Briefly, pLE cells were seeded in a 96-well plate, and then incubated for 24 h in the serum-free DMEM/F12 1:1 medium. The cells were next treated with various concentrations of recombinant CCL4 in a final volume of 100 μL/well. After 48 h of incubation, 10 μM BrdU was added to the cell culture, and the cells were incubated for additional 2 h at 37 °C.

2.11. Cell cycle assay

The pLE cells used in cell cycle assays were seeded (4×10^5 cells) in six-well plates and incubated for 24 h in serum-free medium until cells reached 70–80% confluency. Then, cells were treated with CCL4 in a dose-dependent manner for 48 h at 37 °C in a CO_2 incubator. Supernatants were transferred from culture dishes into collecting tubes and adherent cells detached with trypsin-EDTA. The cells were collected by centrifugation, washed twice with cold PBS, and fixed with chilled 70% ethanol at 4 °C overnight. Cells were then washed twice with PBS, incubated with 10 mg/mL RNase A (Sigma–Aldrich) and 50 mg/mL prolidium iodide (BD Biosciences, Franklin Lakes, NJ, USA) in PBS at room temperature for 30 min in the dark and subjected to flow cytometry using Guava (MERCK, Kenilworth, NJ, USA).

2.12. Western blot analyses

The concentrations of proteins in whole-cell extracts were determined by the Bradford protein assay (Bio-Rad, Hercules, CA, USA) using BSA as the standard. The proteins were denatured, separated by sodium dodecyl sulfate polyacrylamide gel electrophoresis (SDS-PAGE), and then transferred to nitrocellulose membranes. Blots were developed via enhanced chemiluminescence detection (SuperSignal West Pico, Pierce, Rockford, IL, USA) and quantified by measuring the intensity of light emitted from correctly sized bands under ultraviolet light on the ChemiDoc EQ system with the Quantity One software (Bio-Rad). Immunoreactive proteins were detected with goat anti-rabbit polyclonal antibodies against each phosphorylated protein and the corresponding total protein at 1:1000 dilution and were separated by SDS-PAGE in a 10% gel. As a loading control, total protein and α-tubulin (TUBA) were employed to normalize results for detection of target proteins. Multiple exposure of each western blot was performed to ensure linearity of chemiluminescent signals.

2.13. Transwell migration assay

Serum starved pLE cells (1×10^5 cells per 100 mL of serum free DME/F12 1:1 medium) were seeded on 8-mm pore Transwell inserts (Corning, Inc., Corning, NY, USA) and treatments added to each well for 6 h. For evaluation of cells that migrated onto the lower surface, inserts were fixed in methanol for 10 min. The Transwell membranes were then air-dried and stained using hematoxylin (catalog number: HHS32, Sigma-Aldrich, Inc) for 30 min. The insert membranes were washed gently several times with tap water to remove excess stain. The cells on the upper side of the inserts were removed with a cotton swab. The Transwell membranes were removed and placed on a glass slide with the side containing cells facing up, and the slide covered with Permount solution. Migrated cells were counted in five non-overlapping locations, which covered approximately 70% of the insert membrane growth area, using a DM3000 (Leica) microscope. The entire experiment was repeated at least three times.

2.14. Cell migration assay

Cell migration was evaluated using Ibidi migration culture dish inserts according to the manufacturer's protocol (Ibidi, Germany). A 70 mL suspension of pLE cells (2×10^5 cells/mL) was seeded into each well of the culture-inserts and grown overnight to full confluence. After cell starvation for 24 h, the culture inserts were removed from the surface and a 500 μm width cell-free gap between two defined cell patches was created. Cells were incubated with different treatments in fresh culture medium to start the migration process. The migration of cells into the defined cell-free gap (500 μm) was observed, and light microscopy images of the gap fields were acquired after 12 h using a DM3000 Leica light microscope. For assay analyses, the effect of treatment on gap closure was computed.

2.15. Statistical analyses

All quantitative data were subjected to least-squares analysis of variance (ANOVA) via the general linear model procedures of the Statistical Analysis System (SAS Institute Inc., Cary, NC, USA). Western blot data were corrected for differences in sample loading on the basis of total protein or TUBA data as a covariate. All tests of significance were performed with the appropriate error terms according to the expectation of the mean squares for error. Data with a *P*

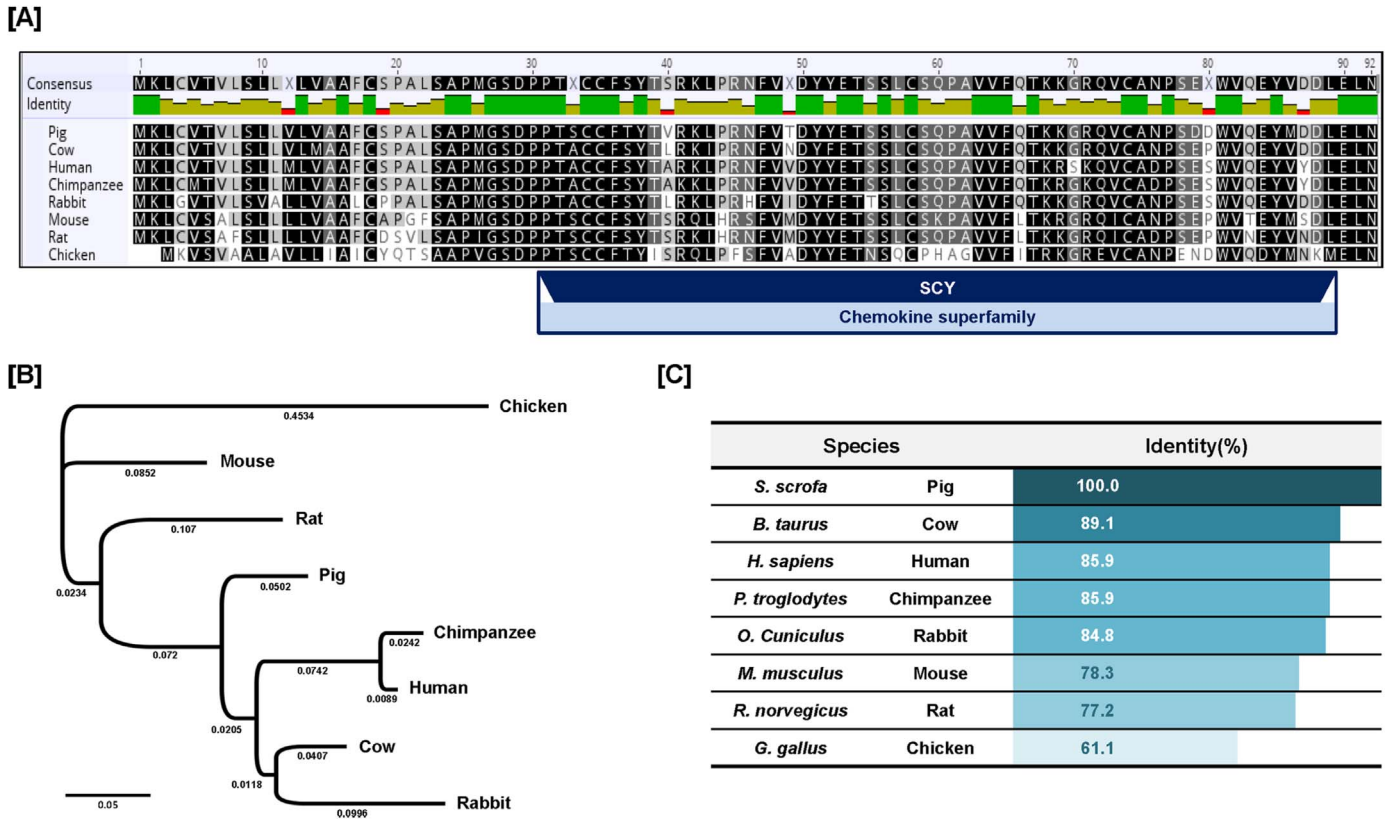

Fig. 1. Multiple-sequence comparisons and a phylogenetic tree based on porcine CCL4 and other CCL4 proteins identified in different species. [A] Multiple-sequence alignment of porcine CCL4 with other CCL4s deposited in GenBank: *Bos taurus* (cow, NP_001068615.1), *Homo sapiens* (human, NP_002975.1), *Pan troglodytes* (chimpanzee, XP_016787457.1), *Oryctolagus cuniculus* (rabbit, NP_001075665.1), *Mus musculus* (mouse, NP_038680.1), *Rattus norvegicus* (rat, NP_446310.1), and *Gallus gallus* (chicken, NP_990051.1). Similar regions in the sequences are boxed. White letters shaded in black indicate that the similarity of this position is 100%, whereas the dark grey letters mean that the similarity of the position is over 75%, but below 100%. The SCY domain involved in the intercrine α family of cytokines was found to be conserved. [B] A phylogenetic tree was constructed by the neighbor-joining method using amino acid sequences from diverse species, and the scale bar indicates the genetic distance among species. [C] A comparison of porcine CCL4 sequence homology to other CCL4s.

value less than or equal to 0.05 were considered significant. Data are presented as a least-squares mean with standard error (SE).

3. Results

3.1. Multiple-sequence comparison and phylogenetic analysis of porcine CCL4

Porcine gene *CCL4* is located on chromosome 12, is composed of three exons, and its full-length cDNA sequence (1322 bp) encodes a protein of 92 amino acid residues. The *CCL4* gene from pigs and other species contains the conserved SCY domain belonging to the intercrine alpha family of cytokines involved in cell-specific chemotaxis, cell growth, and inflammatory responses (Fig. 1A). Eight CCL4s from vertebrates and invertebrates were chosen and served for construction of a phylogenetic tree by the neighbor-joining method (Fig. 1B). Porcine CCL4 appeared to associate more closely with mammalian and ruminant CCL4s than those from other species. In particular, the porcine CCL4 protein shows high similarities (61.1–89.1%) with CCL4s identified in other species, such as 85.9% similarity with human and chimpanzee CCL4, 89.1% similarity with cow CCL4, 84.8% similarity with rabbit CCL4, 78.3% similarity with mouse CCL4, 77.2% similarity with rat CCL4, and 61.1% similarity with chicken CCL4 (Fig. 1C).

3.2. Cell-specific expression of CCL4 and its receptor CCR5 in the porcine endometrium during estrus cycle and early pregnancy

Quantitative RT-PCR and *in situ* hybridization analyses showed distributions of mRNA expression of *CCL4* and *CCR5* in porcine endometrial tissues during the estrus cycle and early pregnancy (Fig. 2). The expression of porcine *CCL4* mRNA in the endometrium decreased by half ($P < 0.05$) on day 15 of the estrus cycle as compared to day 9 (Fig. 2A). In contrast, *CCL4* expression increased 2.8-fold ($P < 0.01$), 3.3-fold ($P < 0.01$), and 3.2-fold ($P < 0.001$) on days 14, 20, and 30 of pregnancy, respectively, in the porcine endometrium. And, the expression of *CCR5* decreased in porcine endometrium on days 12 and 15 of the estrous cycle compared to expression on day 9 of the estrous cycle (Fig. 2B). However, *CCR5* mRNA expression increased gradually (1.2- to 3.7-fold; $P < 0.05$, $P < 0.01$, and $P < 0.001$) from day 9 to day 30 of pregnancy. The relatively high level of expression of mRNAs for *CCL4* and *CCR5* was detected mainly in uterine GE and LE of the porcine endometrium from day 14 to day 30 of pregnancy (Fig. 2C and D).

3.3. Effects of CCL4 on proliferation and cell cycle phases of pLE cells

To explore the functions of CCL4 in the porcine endometrium during pregnancy, we performed cell proliferation and cell cycle analyses on pLE cells isolated from porcine uterine luminal epithelial cells on day 12 of pregnancy (Fig. 3). Treatment of pLE cells with CCL4 in a dose-dependent manner significantly increased cellular proliferation: by ~ 126% ($P < 0.05$), 134% ($P < 0.05$), 151% ($P < 0.01$), 192% ($P < 0.01$), and 188% ($P < 0.05$) at 5, 10, 25, 50, and 100 ng/mL CCL4, respectively (Fig. 3A). In addition, CCL4 activated phosphorylation of cyclin D1, as well as PCNA protein in pLE cells as concentrations of CCL4 increased (Fig. 3B and C). In addition, incubation of pLE cells with CCL4, the distribution of cells changed gradually due to an increase in the number of cells at the G2–M transition according to

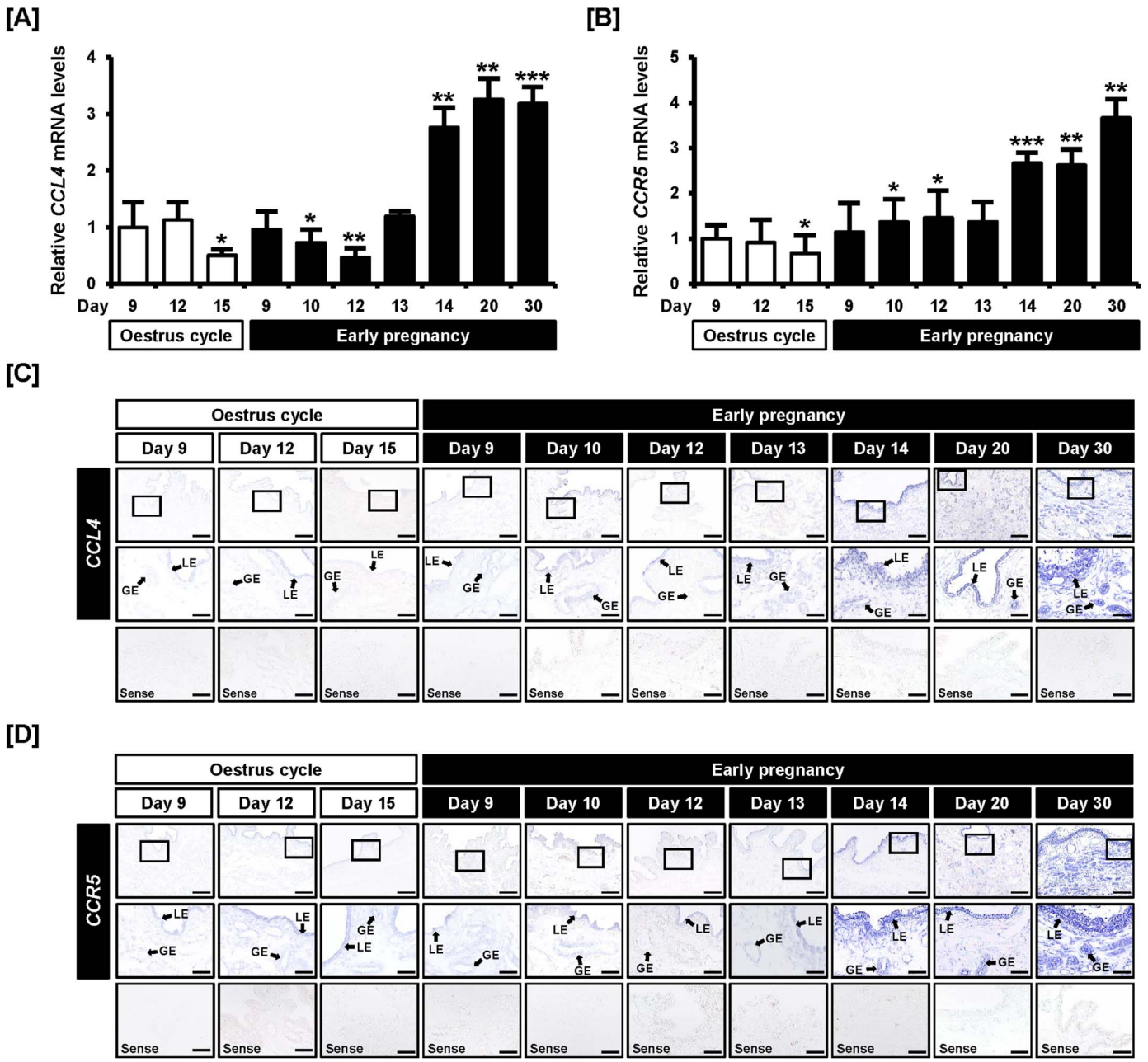

Fig. 2. Relative expression and localization of *CCL4* and *CCR5* mRNAs in the porcine endometrium during the estrous cycle and early pregnancy. [A and B] Differential expression of *CCL4* [A] and *CCR5* [B] mRNAs was determined using quantitative RT-PCR in porcine endometrium during the estrous cycle (days 9, 12, and 15) and early pregnancy (days 9, 10, 12, 13, 14, 20, and 30). Expression of *CCL4* and *CCR5* mRNAs was normalized to *GAPDH*. Data were analyzed and compared to data from day 9 of the estrous cycle in pigs. Asterisks indicate a significant difference in the expression (***$P < 0.001$, **$P < 0.01$, and *$P < 0.05$). [C and D] Localization of *CCL4* [C] and *CCR5* [D] mRNAs was analyzed in porcine endometrium by *in situ* hybridization during the estrous cycle and early pregnancy. Legend: GE, glandular epithelium; LE, luminal epithelium. The scale bar is 50 μm (the first horizontal panels and sense) and 20 μm (the second horizontal panels).

flow-cytometric analyses with a propidium iodide dye (Fig. 3D). These results indicated that CCL4 increased proliferation of pLE cells.

3.4. Signal transduction stimulated by CCL4 in pLE cells

To determine CCL4-regulated signaling pathways, we performed an immunoblot assay on CCL4-treated pLE cells by means of PI3K and MAPK signaling molecules, which are closely associated with cellular proliferation (Fig. 4). Treatment with CCL4 activated phosphorylation of signaling proteins AKT, P70S6K, and S6 in pLE cells in a dose-dependent manner (0, 10, 25, and 50 ng/mL) as illustrated in Fig. 4A–C. Besides, in the MAPK pathways, phosphorylation of ERK1 and ERK2, JNK, and P38 proteins significantly increased in the CCL4-treated pLE cells in response to a high concentration (Fig. 4D–F). Then, we confirmed the effects of CCL4 on the proliferation of pLE cells with pharmacological inhibitors of PI3K and MAPK pathways (Fig. 5A). The CCL4-induced proliferation of pLE cells was decreased by cotreatment with wortmannin (PI3K inhibitor), U0126 (ERK1 and -2 inhibitor), SP600125 (JNK inhibitor), or SB203580 (P38 inhibitor). Moreover, the CCL4-driven upregulation of proteins p-AKT, P70S6K, and S6 in pLE cells was completely suppressed by cotreatment with wortmannin (Fig. 5B–D). Their activities also decreased in pLE cells in response to the inhibitors of MAPK pathways. The CCL4-activated ERK1 and -2 phosphorylation was decreased not only by wortmannin, SP600125, or SB203580 but also by U0126 (Fig. 5E). Although the phosphorylation of JNK was downregulated by the MAPK inhibitors

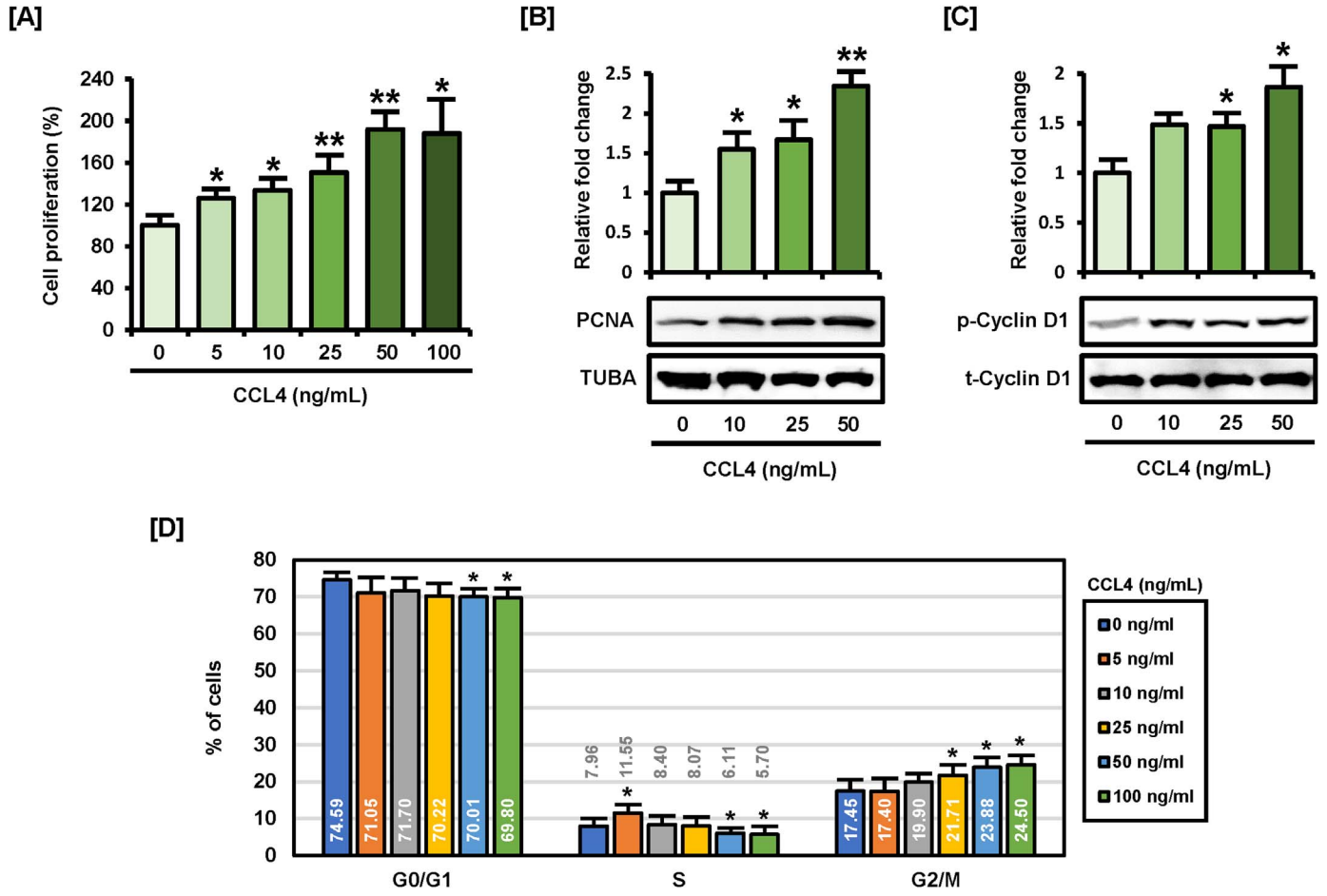

Fig. 3. Effects of CCL4 on proliferation and cell cycle of pLE cells. [A] Proliferation of porcine uterine luminal epithelial (pLE) cells in response to various doses of CCL4 (0, 5, 10, 25, 50, and 100 ng/mL). Relative proliferation is expressed as a percentage ratio relative to vehicle-treated pLE cells (100%). [B and C] Western blot analyses revealed abundances of PCNA [B] and phosphorylated cyclin D1 (p-cyclin D1) [C] in pLE cells treated with CCL4 (0, 10, 25, and 50 ng/mL). The intensity of the immunoblots was calculated to normalize the data on PCNA to α-tubulin (TUBA) and to normalize p-Cyclin D1 data to total cyclin D1. All error bars represent standard error of the mean (SEM) of representative experiments conducted in triplicate. [D] The proportion of cells in various stages of the cell cycle were analyzed by flow cytometry after propidium iodide (PI) staining to determine effects of CCL4-treated progression of pLE cells through the cell cycle. Asterisks indicate a significant difference from vehicle-treated pLE cells (**$P < 0.01$ and *$P < 0.05$).

compared to the CCL4-treated pLE cells, a combination of CCL4 and wortmannin highly increased the JNK activity (Fig. 5F). As in proteins ERK1 and ERK2, phosphorylation of P38 elevated by CCL4 was inhibited by cotreatment with one of the four inhibitors as compared to the CCL4 only-treated pLE cells (Fig. 5G). Lastly, cyclin D1 phosphorylation in the CCL4-treated pLE cells was found to be completely blocked by each inhibitor (Fig. 5H). These results indicated that the blockage of PI3K and MAPK activities suppressed the abilities of CCL4 to activate the proliferation of (and signal transduction in) pLE cells.

3.5. Suppression of ER stress in response to CCL4 in pLE cells

To determine the effects of CCL4 on ER stress, we performed a cell proliferation assay on pLE cells in response to treatment with tunicamycin (an ER stress inducer), CCL4, or their combination (Fig. 6A). Tunicamycin decreased the proliferation of pLE cells ($P < 0.01$), but cotreatment with CCL4 recovered the proliferative properties of pLE cells. In accordance with ER stress, glucose-regulated protein 78 kDa (GRP78), which is crucial for regulation of the unfolded protein response (UPR), was strongly activated in the tunicamycin-treated pLE cells (Fig. 6B). By contrast, the combined treatment of pLE cells with tunicamycin and CCL4 decreased the GRP78 protein levels as compared to treatment with tunicamycin alone. In addition, the three ER stress sensors—inositol-requiring protein 1α (IRE1α), activating transcription factor 6α (ATF6α), and PRKR-like ER kinase (PERK)—were stimulated in the pLE cells by tunicamycin, but their activities were downregulated by cotreatment with CCL4 (Fig. 6C–E). In accordance with the three ER stress sensor activities, the downstream signaling molecule PERK, eukaryotic translation initiation factor 2α (eIF2α), and a transcription factor called growth arrest and DNA damage gene 153 (GADD153, also known as CHOP) were induced in the tunicamycin-treated pLE cells whereas their amounts returned to basal levels in response to CCL4 (Fig. 6F and D). These results revealed that CCL4 suppressed ER stress, thereby improving viability of pLE cells.

3.6. Inhibitory effects of CCL4 on lipopolysaccharide (LPS)-induced inflammation in pLE cells

Next, we studied the effects of CCL4 on LPS-induced inflammation in pLE cells by an immunoblot assay as illustrated in Fig. 7. Treatment with LPS stimulated an adaptor protein called myeloid differentiation primary response 88 (MyD88) approximately 1.2-fold ($P < 0.05$), thus activating the transcription factor nuclear factor kappa B (NF-κB) in pLE cells compared to untreated pLE cells (Fig. 7A). Nonetheless, MyD88 protein levels returned to baseline after CCL4 treatment. Because MyD88 next signals through interleukin 1 receptor–associated kinase (IRAK), we quantified the phosphorylation of IRAK1 directly regulated by MyD88 in pLE cells in response to LPS and CCL4 treatment (Fig. 7B). Although phosphorylation of IRAK1 was activated in the LPS-treated pLE cells (1.3-fold, $P < 0.05$), this phosphorylation was decreased by cotreatment with CCL4. Moreover, activity of a

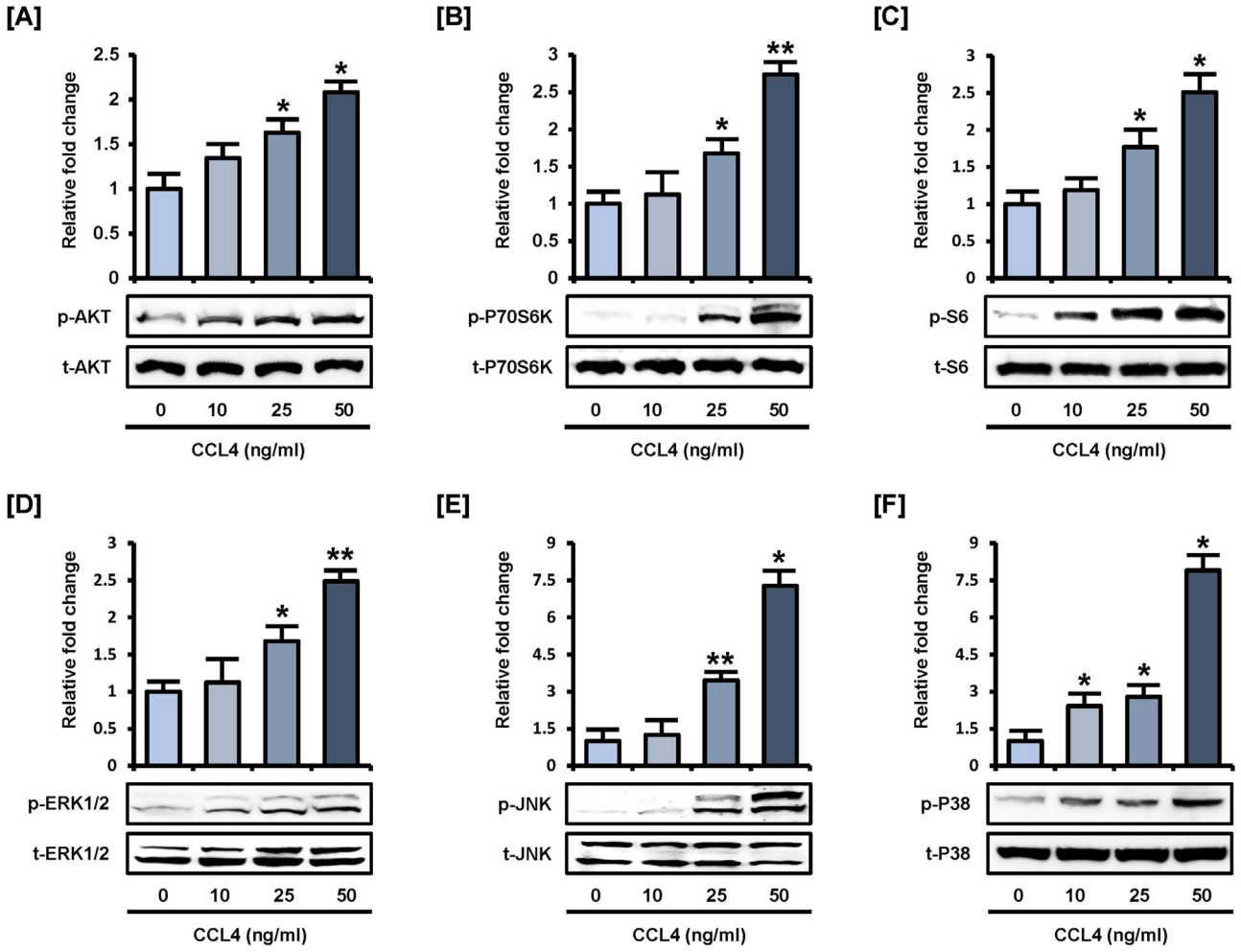

Fig. 4. Stimulatory effects of CCL4 on activation of PI3K and MAPK pathways in pLE cells. [A to F] Western blot analyses indicate the abundances of p-AKT [A], p-P70S6K [B], p-S6 [C], p-ERK1/2 [D], p-JNK [E], and p-P38 [F] proteins in pLE cells treated with CCL4. The intensity of immunoblots was calculated to normalize data for each phosphoprotein to the corresponding total protein. Asterisks indicate a significant difference from vehicle-treated pLE cells (**$P < 0.01$ and *$P < 0.05$).

downstream player of the LPS-regulated TLR4 pathway—transforming growth factor β-activated kinase 1 (TAK1)—increased approximately 1.5-fold ($P < 0.01$) in LPS-treated pLE cells compared to control cells, whereas this activity returned to the basal levels (Fig. 7C). Similarly, treatment of pLE cells with LPS increased the phosphorylation of IκB kinase alpha and beta subunits (IKKα/β), and cotreatment with LPS and CCL4 inactivated the phosphorylation of IKKα/β (Fig. 7D). Furthermore, the NF-κB activation in pLE cells by LPS treatment (4.2-fold, $P < 0.01$) was attenuated by cotreatment with CCL4 (Fig. 7E). These results implied that the treatment of pLE cells with CCL4 inhibited the signs of LPS-induced inflammation.

3.7. Effects of inhibition of CCR5 on proliferation of pLE cells

To investigate the role of CCR5 in proliferation of pLE cells and cell signaling pathways, we used Maraviroc that is an antagonist of CCR5 (Fig. 8). The CCL4-induced proliferation of pLE cells returned to a basal level following treatment with Maraviroc (Fig. 8A). In addition, treatment of pLE cells with Maraviroc alone decreased their proliferation approximately 25% ($P < 0.01$) compared to untreated cells. The CCL4-activated phosphorylation of AKT, P70S6K and S6 decreased significantly when pLE cells were subjected to the combined effects of CCL4 and CCR5 compared to CCL4 alone (Fig. 8B-D). Also, Maraviroc also reduced phosphorylation of AKT and P70S6K in pLE compared to control cells. Furthermore, in the MAPK pathways, the phosphorylation of ERK1 and ERK2, JNK, and P38 proteins decreased significantly in pLE cells treated with CCL4 and CCR5 compared to treatment with CCL4 alone (Fig. 8E-G). These results indicate that CCR5 regulates CCL4-activated proliferation and associated signal transduction pathways in pLE cells.

3.8. Effects of CCL4 on interactions between pTr and pLE cells during early pregnancy

In order to determine the functional role of CCL4 in peri-implantation conceptuses, we performed proliferation assays using porcine trophectoderm (pTr) cells established from day 12 pregnant gilts (Fig. 9A). Treatment of pTr cells with CCL4 (0–50 ng/mL) increased their proliferation about 153% ($P < 0.05$) and 172% ($P < 0.01$) at 25 and 50 ng/mL, respectively. In addition, CCL4 increased migration of pTr cells by 142% ($P < 0.05$) and 140% at 10 and 25 ng/mL, respectively, whereas it decreased migration of pTr cells at 50 ng/mL (Fig. 9B). In contrast, CCL4 (50 ng/mL) strongly increased migration of pLE cells by about 300% ($P < 0.01$) (Fig. 9C). Next, we analyzed cell to cell migration between pTr and pLE cells in response to CCL4 using 2D culture-insert dishes (Fig. 9D). Relative wound width between pTr and pLE cells decreased 18% ($P < 0.05$) and 29% ($P < 0.05$) at 50 and 100 ng/mL of CCL4. After that, we determined expression of implantation-related genes previously identified in CCL4-treated pTr and pLE cells (Fig. 9E-N). In pTr cells, the expression of mRNAs for *adiponectin receptor 1 (ADIPOR1), ADIPOR2, epidermal growth factor receptor* (*EGFR*), fibroblast growth factor receptor 1 (FGFR1) and *vascular*

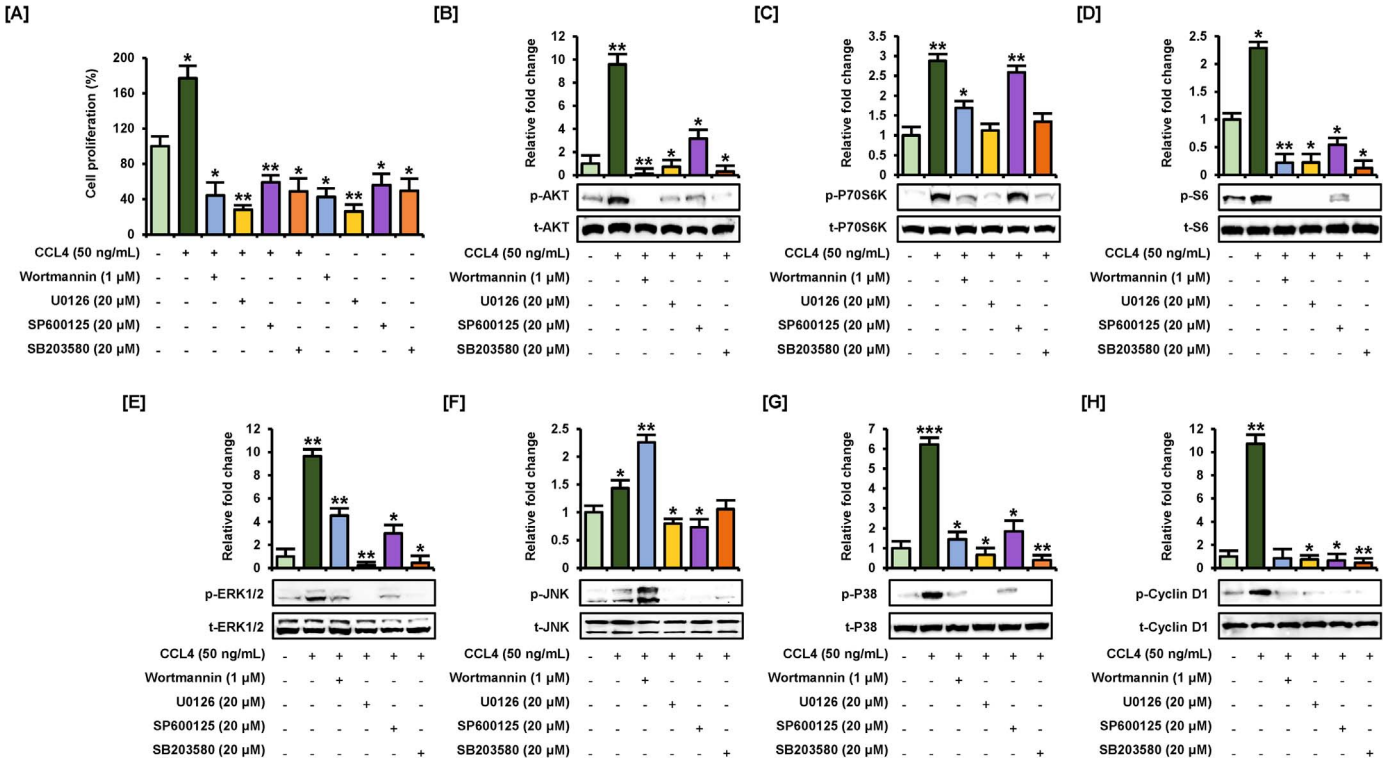

Fig. 5. Effects of CCL4 during cotreatment with inhibitors of PI3K or MAPKs on the proliferation and signal transduction in pLE cells. [A] Proliferation of pLE cells was analyzed during treatment with CCL4 (50 ng/mL), or cotreatment with CCL4 plus wortmannin (1 μM), U0126 (20 μM), SP600125 (20 μM), or SB203580 (20 μM). Relative proliferation of pLE cell presented as a percentage ratio relative to proliferation of vehicle-treated pLE cells (100%). [B to H] Western blot analyses indicate the abundances of p-AKT [B], p-P70S6K [C], p-S6 [D], p-ERK1/2 [E], p-JNK [F], p-P38 [G], and p-Cyclin D1 [H] proteins in pLE cells treated with CCL4 or in pLE cells cotreatment with each inhibitor. The intensity of immunoblots was calculated to normalize abundance of each phosphoprotein to the corresponding total protein. Asterisks denote a significant difference from vehicle-treated pLE cells (***$P < 0.001$, **$P < 0.01$, and *$P < 0.05$).

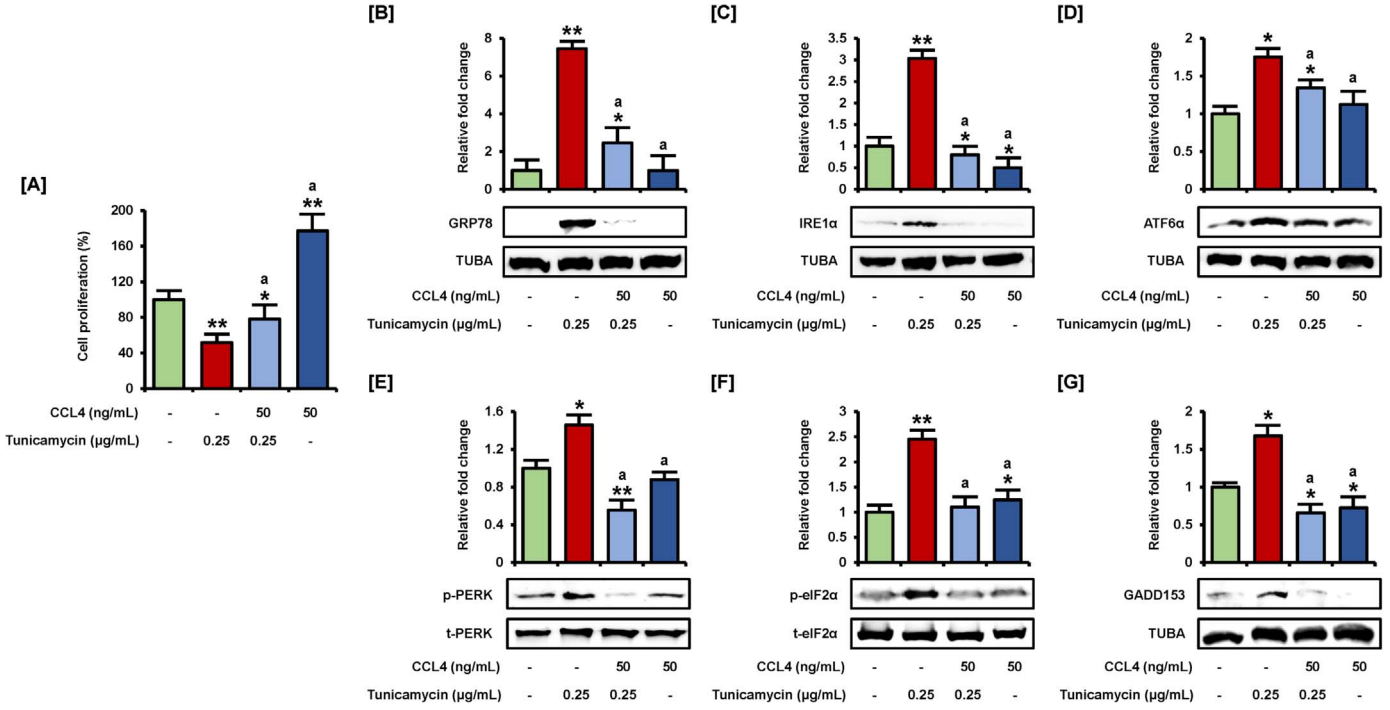

Fig. 6. Effects of CCL4 on tunicamycin-stimulated ER stress in pLE cells. [A] Proliferation of pLE cells was analyzed during treatment with tunicamycin (0.25 μg/mL), CCL4 (50 ng/mL), or their combination for 48 h. Relative proliferation of pLE cells is presented as the ratio relative to vehicle-treated pLE cells (100%). [B to G] Western blot analyses reveals the abundances of GRP78 [B], IRE1α [C], ATF6α [D], p-PERK [E], p-eIF2α [F], and GADD153 [G] proteins in pLE cells during treatment with tunicamycin, CCL4, or their combination for 24 h. The intensity of immunoblots was calculated to normalize abundance of each target protein to the respective total protein or TUBA. Asterisks indicate a significant difference from vehicle-treated pLE cells (**$P < 0.01$ and *$P < 0.05$). Lowercase letter (a) indicates a statistically significant change ($P < 0.05$) compared with effects of tunicamycin alone.

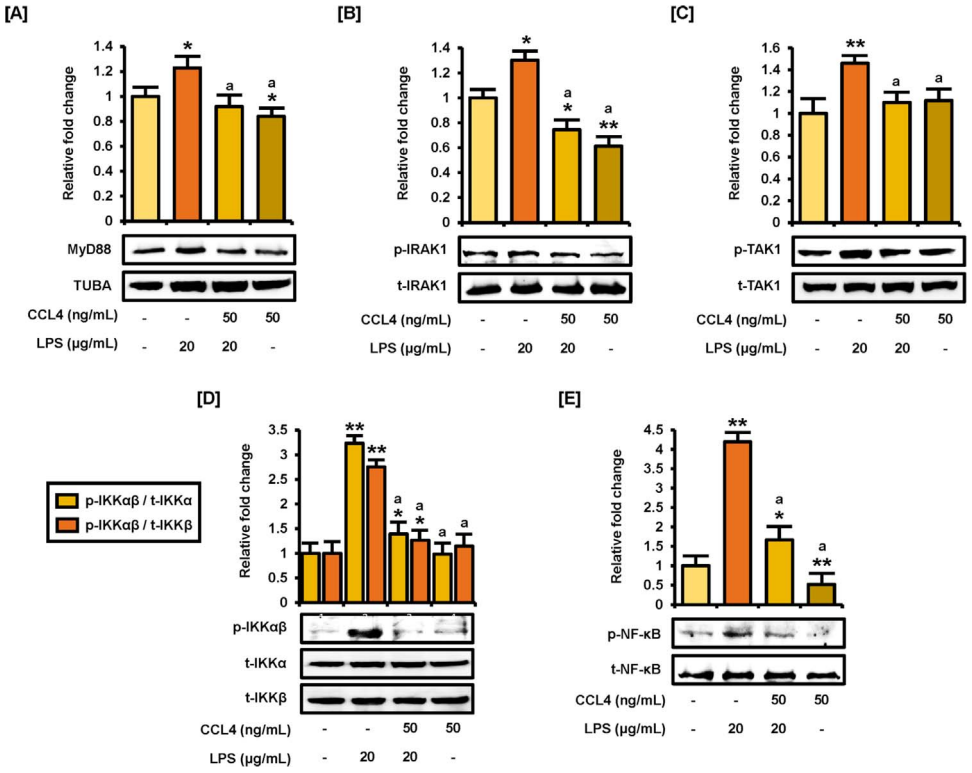

Fig. 7. Effects of CCL4 on LPS-induced inflammation in pLE cells. [A to E] Western blot analyses of the abundances MyD88 [A], IRAK1 [B], TAK1 [C], IKKα/β [D], and NF-κB [E] proteins in pLE cells treated with LPS (20 μg/mL), CCL4 (50 ng/mL), or their combination for 24 h. The intensity of immunoblots was calculated to normalize the abundance of each target protein to the corresponding total protein or TUBA. Asterisks indicate a significant difference from vehicle-treated pLE cells (**P < 0.01 and *P < 0.05). Lowercase letter (a) indicates a statistically significant change (P < 0.05) compared with effects of LPS alone.

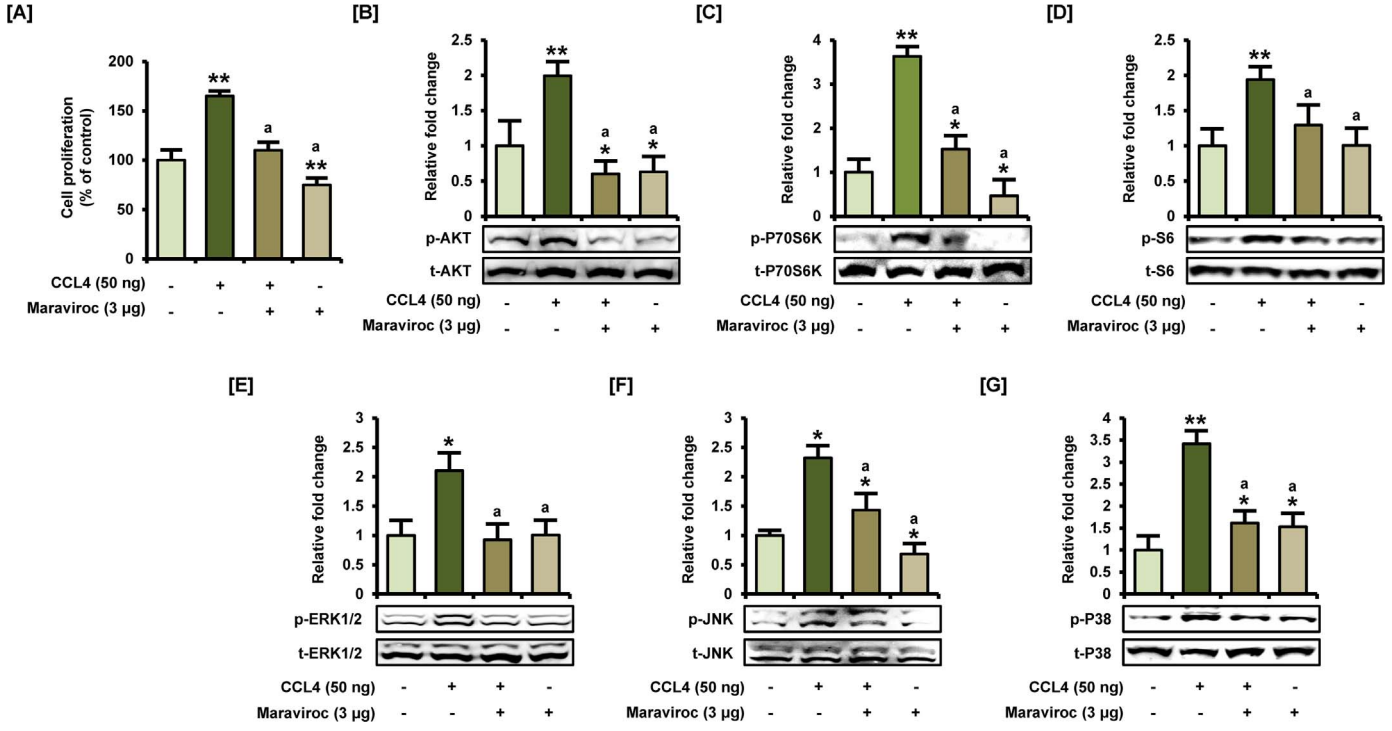

Fig. 8. Effects of CCR5 antagonist on CCL4-induced proliferation and signal transduction molecules in pLE cells. [A] Proliferation of pLE cells was analyzed during treatment with Maraviroc (3 μg/mL), CCL4 (50 ng/mL), or their combination for 48 h. Relative cellular proliferation is presented as a percentage ratio relative to vehicle-treated pLE cells (100%). [B to G] Western blot analyses indicate abundances of p-AKT [B], p-P70S6K [C], p-S6 [D], p-ERK1/2 [E], p-JNK [F], and p-P38 [G] proteins in pLE cells during treatment with Maraviroc, CCL4, or their combination for 24 h. The intensity of immunoblots was calculated to normalize abundance of each phosphoprotein to the corresponding total protein. Asterisks denote a significant difference from vehicle-treated pLE cells (**P < 0.01, and *P < 0.05). Lowercase letter (a) indicates a statistically significant change (P < 0.05) compared with effects of Maraviroc alone.

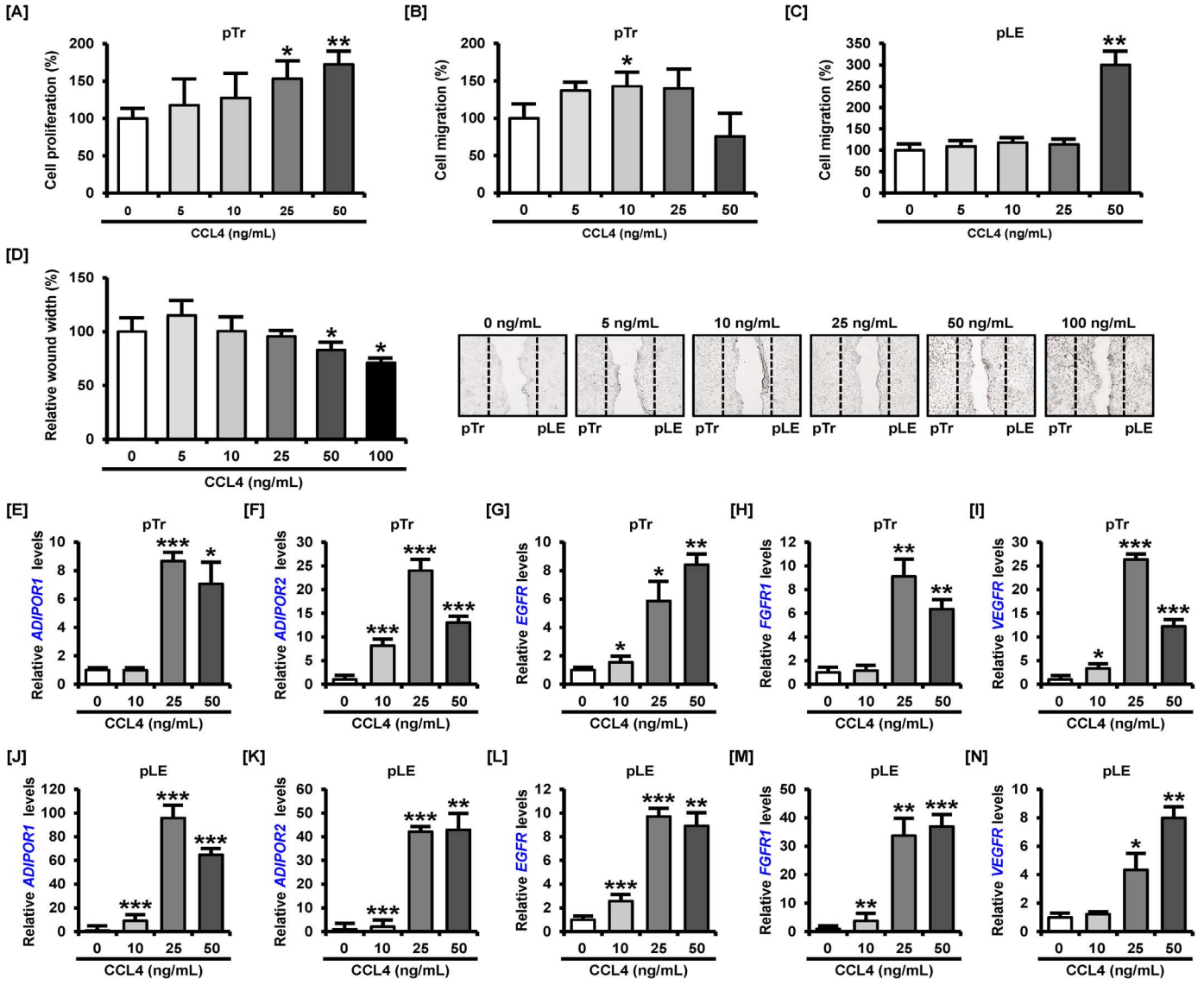

Fig. 9. Effects of CCL4 on interactions between peri-implantation conceptuses and maternal endometrium during the implantation period. [A] Proliferation of pTr cells was analyzed during treatment with CCL4 in a dose-dependent manner (0, 5, 10, 25 and 50 ng/mL) for 48 h. Relative proliferation of cells is presented as a percentage ratio relative to vehicle-treated pTr cells (100%). [B and C] Migration of pTr [B] and pLE [C] cells was analyzed using Transwell migration plates during treatment with CCL4 (0, 5, 10, 25 and 50 ng/mL) for 6 h. Relative migration of cells is presented as a percentage ratio relative to vehicle-treated cells (100%). [E to I] Relative expression of mRNAs for porcine implantation-related genes *ADIPOR1* [E], *ADIPOR2* [F], *EGFR* [G], *FGFR1* [H] and *VEGFR* [I] in pTr cells in response to CCL4. The expression of target genes was normalized to GAPDH. Data were analyzed to compare treated versus untreated pTr cells. [J to N] Relative expression of *ADIPOR1* [J], *ADIPOR2* [K], *EGFR* [L], *FGFR1* [M] and *VEGFR* [N] mRNAs in pLE cells in response to CCL4. The expression of target genes was normalized to GAPDH. Data were analyzed to compare effects relative to untreated pLE cells. Asterisks denote a significant difference from vehicle-treated cells (***$P < 0.001$, **$P < 0.01$, and *$P < 0.05$).

endothelial growth factor receptor (*VEGFR*) increased in response to treatment with CCL4 ($P < 0.05$, $P < 0.01$ and $P < 0.001$) (Fig. 9E-I). Also, CCL4 activated all of the implantation-related target genes in pLE cells in a dose-dependent manner ($P < 0.05$, $P < 0.01$ and $P < 0.001$) (Fig. 9J-N). These results indicate that CCL4 enhanced implantation between peri-implantation conceptuses and maternal endometrium during early pregnancy.

4. Discussion

Results of this study suggest that CCL4 improved development of the porcine endometrium *in vivo* and *in vitro* during early pregnancy. Treatment with CCL4 activated PI3K and MAPK signal transduction stimulating proliferation of pLE cells and suppressed ER stress and inflammation by regulating UPR and NF-κB signaling proteins as presented in Fig. 10. Also, CCL4 increased migration between pTr and pLE cells through activation of implantation-related genes. These results support our hypothesis that CCL4 promotes maternal–fetal interactions in early pregnancy.

CCL4 (also known as macrophage inflammatory protein 1β) is one of the members of the CC chemokine subfamily and is deeply involved in the progression of chronic diseases, infectious diseases, and cancers and in reproductive events by recruiting NK cells, monocytes, and other immune cells (Menten et al., 2002). Chemokines and cytokines are important for extensive communication between embryonic and endometrial cells in the implantation period and early pregnancy (Guzeloglu-Kayisli et al., 2009; Ramhorst et al., 2016). According to some studies, CCL4 not only regulates the development of endometrial tissue in the secretory phase of the endometrial cycle for preparing pregnancy but also stimulates the migration of trophoblast cells at the maternal–fetal interface (Hannan et al., 2006; Kitaya et al., 2003). In addition, the expression of CCL4 mRNA and protein in humans is upregulated in choriodecidual tissues during term labor in comparison with preterm labor (Hamilton et al., 2013). Moreover, high levels of

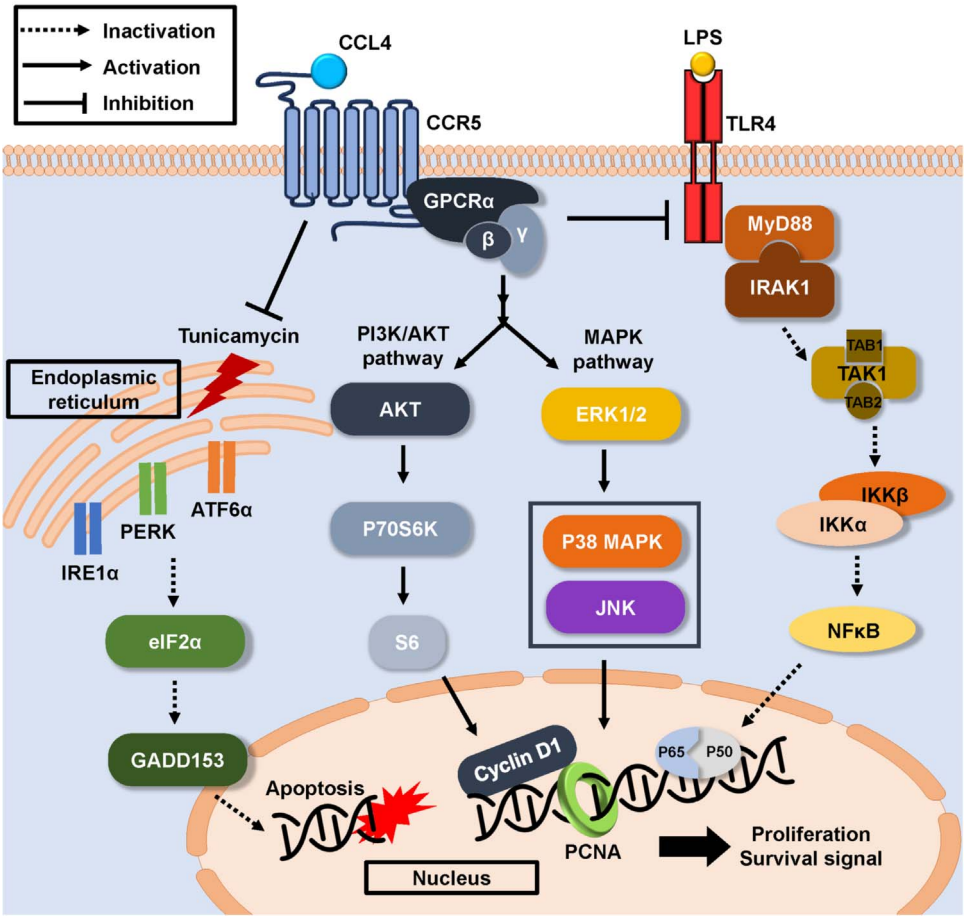

Fig. 10. Hypothetical illustration of CCL4-mediated signal transduction in pLE cells. CCL4 activates PI3K and MAPK pathways through CCR5, thereby improving the proliferation and survival of pLE cells. Treatment with CCL4 prevents tunicamycin-induced cell death via effects on UPR-regulatory proteins. In addition, treatment with CCL4 inhibits LPS-triggered inflammation in pLE cells by regulating NF-κB signaling proteins. Overall, CCL4 may play an important role in development of the porcine endometrium in the early gestational period.

CCL4 may serve as a potential biomarker for predicting implantation competence in patients undergoing *in vitro* fertilization just as secreted phosphoprotein 1, which is a predictor of uterine receptivity (Gnainsky et al., 2010). To exert its biological actions, CCL4 commonly binds to G protein–coupled cell surface receptors such as CCR1 and CCR5 (Di Marzio et al., 2005). The expression of human CCR5 is present in the epithelial and stromal regions of the uterus throughout the endometrial cycle and in the blastocyst (Dominguez et al., 2003; Mulayim et al., 2003). In particular, our previous study has shown that the expression of *CCR1* mRNA increases in the porcine endometrium during early pregnancy (Jeong et al., 2017). In the present study, we determined the spatial and temporal patterns of expression of *CCL4* and *CCR5* in the porcine endometrium during the estrus cycle and early gestational period. Both genes were found to be widely expressed in the GE and LE of the endometrium in pigs during early pregnancy. In addition, incubation with CCL4 increased the proliferation of pLE cells via activation of PCNA, PI3K–AKT, and MAPK signal transduction cascades, which are closely associated with cell growth, migration, and differentiation. Results of various studies support our results revealing the stimulatory effects of the PI3K–AKT pathway on the successful induction of decidualization during pregnancy and on ERK1 and −2 MAPK–mediated proliferation of the endometrial cells (Fabi et al., 2017; Jabbour and Boddy, 2003). Moreover, suppression of CCR5 inhibited CCL4-induced proliferation of pLE cells by decreasing phosphorylation of PI3K and MAPK cell signaling molecules. Also, treatment of cells with CCL4 enhanced interactions between peri-implantation conceptuses and maternal endometrium in pigs by increasing *ADIPOR1*, *ADIPOR2*, *EGFR*, *FGFR1*, and *VEGFR*. All target genes were enhancers or indicators of implantation of blastocysts in pigs (Jeong et al., 2016, 2014; Lim et al., 2017a, 2017b).

Accumulation of unfolded or misfolded proteins within ER cisternae under both physiological and pathological conditions leads to ER stress and enhances the accompanying UPR (Hetz, 2012). During pregnancy, ER stress is one of the key factors that provoke intrauterine growth restriction (Yung et al., 2008), pre-eclampsia (Burton and Yung, 2011), preterm birth (Liong and Lappas, 2014), and fetal loss (Liu et al., 2011). For instance, the expression of PERK, eIF2α, GRP78, and GADD153 is activated in the placenta of women with severe pre-eclampsia as compared to healthy women (Fu et al., 2015). In addition, inactivation of IRE1α and X-box–binding protein 1 abrogates placentation and embryogenesis in mice (Iwawaki et al., 2009). Although ER stress causes death of pLE cells by activating cleavage of caspase 3, treatment with CCL2 restores cell survival with downregulation of ER stress–regulatory proteins (Lim et al., 2018). On the other hand, the involvement of CCL4 in ER stress is poorly understood at present. In this study, tunicamycin-induced ER stress decreased the proliferation of pLE cells, and cotreatment with CCL4 recovered the proliferative activities of the pLE cells and attenuated the activation of UPR-related proteins. These results indicate that CCL4 counteracts ER stress under the influence of stressful stimuli in the porcine endometrium during early pregnancy.

Maternal infection is one of the major causes of intrauterine fetal death and preterm birth during pregnancy (Aisemberg et al., 2007; Xu et al., 2007). Infection-driven intrauterine inflammation mediated by LPS induces oxidative stress in the mouse placenta and nitric oxide production in maternally derived fluids such as serum and amniotic

fluid (Xu et al., 2007). Moreover, LPS activates production of prostaglandins and the expression of cyclooxygenase 2 in the mouse uterus, thus leading to pregnancy complications including fetal resorption during early pregnancy (Aisemberg et al., 2007). Maternally administered LPS decreases fetal survival via cell death in the periventricular white matter region of the brain accompanying an increase of interleukin-1β (IL-1β) levels in guinea pigs (Harnett et al., 2007). Furthermore, LPS induces neural-tube defects and fetal growth restriction by upregulating MyD88, tumor necrosis factor α, IL-1β, and NF-κB in the mouse placenta (Zhao et al., 2014). In the present study, treatment of pLE cells with LPS provoked an inflammatory response through activation of NF-κB signaling. In contrast, cotreatment with CCL4 reduced the activities of NF-κB signaling molecules such as MyD88, IRAK1, TAK1, IKKα/β, and NF-κB. These results suggest that treatment with CCL4 is effective at preventing the LPS-induced inflammation signs in pLE cells.

5. Conclusions

In summary, porcine CCL4 shares high sequence similarity (~ 85.9%) with the human CCL4 protein. Abundant expression of porcine CCL4 in epithelial cells of the endometrium in early pregnancy and stimulatory effects of CCL4 on pLE cells via PI3K–AKT and MAPK pathways suggest that CCL4 promotes successful implantation and placentation. In addition, treatment with CCL4 attenuates tunicamycin-induced ER stress and LPS-induced inflammation signs in pLE cells. Moreover, CCL4 increases migration and implantation-related genes in pTr and pLE cells. Thus, CCL4 may enhance conceptus-endometrial interactions and prevent peri-implantation failure of blastocyst development and survival during early pregnancy in pigs.

Acknowledgements

This research was funded by Basic Science Research Program (2015R1D1A1A01059331) through the National Research Foundation of Korea (NRF) funded by the Ministry of Education, Science, and Technology.

Conflict of interest

The authors have no conflicts of interest to declare.

Appendix A. Supporting information

Supplementary data associated with this article can be found in the online version at doi:10.1016/j.ydbio.2018.06.022.

References

Aisemberg, J., Vercelli, C., Billi, S., Ribeiro, M.L., Ogando, D., Meiss, R., McCann, S.M., Rettori, V., Franchi, A.M., 2007. Nitric oxide mediates prostaglandins' deleterious effect on lipopolysaccharide-triggered murine fetal resorption. Proc. Natl. Acad. Sci. USA 104, 7534–7539.
Bazer, F.W., Spencer, T.E., Johnson, G.A., Burghardt, R.C., Wu, G., 2009. Comparative aspects of implantation. Reproduction 138, 195–209.
Borroni, E.M., Bonecchi, R., Buracchi, C., Savino, B., Mantovani, A., Locati, M., 2008. Chemokine decoy receptors: new players in reproductive immunology. Immunol. Investig. 37, 483–497.
Burton, G.J., Yung, H.W., 2011. Endoplasmic reticulum stress in the pathogenesis of early-onset pre-eclampsia. Pregnancy Hypertens. 1, 72–78.
Cha, J., Dey, S.K., 2014. Cadence of procreation: orchestrating embryo-uterine interactions. Semin. Cell Dev. Biol. 34, 56–64.
Chen, X., Li, A., Chen, W., Wei, J., Fu, J., Wang, A., 2015. Differential gene expression in uterine endometrium during implantation in pigs. Biol. Reprod. 92, 52.
Di Marzio, P., Dai, W.W., Franchin, G., Chan, A.Y., Symons, M., Sherry, B., 2005. Role of Rho family GTPases in CCR1- and CCR5-induced actin reorganization in macrophages. Biochem. Biophys. Res. Commun. 331, 909–916.
Dominguez, F., Galan, A., Martin, J.J., Remohi, J., Pellicer, A., Simon, C., 2003. Hormonal and embryonic regulation of chemokine receptors CXCR1, CXCR4, CCR5 and CCR2B in the human endometrium and the human blastocyst. Mol. Hum. Reprod. 9, 189–198.
Du, M.R., Wang, S.C., Li, D.J., 2014. The integrative roles of chemokines at the maternal-fetal interface in early pregnancy. Cell. Mol. Immunol. 11, 438–448.
Fabi, F., Grenier, K., Parent, S., Adam, P., Tardif, L., Leblanc, V., Asselin, E., 2017. Regulation of the PI3K/Akt pathway during decidualization of endometrial stromal cells. PLoS One 12, e0177387.
Felsenstein, J., 1985. Confidence limits on phylogenies: an approach using the bootstrap. Evolution 39, 783–791.
Fu, J., Zhao, L., Wang, L., Zhu, X., 2015. Expression of markers of endoplasmic reticulum stress-induced apoptosis in the placenta of women with early and late onset severe pre-eclampsia. Taiwan J. Obstet. Gynecol. 54, 19–23.
Gascuel, O., Steel, M., 2006. Neighbor-joining revealed. Mol. Biol. Evol. 23, 1997–2000.
Gnainsky, Y., Granot, I., Aldo, P.B., Barash, A., Or, Y., Schechtman, E., Mor, G., Dekel, N., 2010. Local injury of the endometrium induces an inflammatory response that promotes successful implantation. Fertil. Steril. 94, 2030–2036.
Guzeloglu-Kayisli, O., Kayisli, U.A., Taylor, H.S., 2009. The role of growth factors and cytokines during implantation: endocrine and paracrine interactions. Semin. Reprod. Med. 27, 62–79.
Hamilton, S.A., Tower, C.L., Jones, R.L., 2013. Identification of chemokines associated with the recruitment of decidual leukocytes in human labour: potential novel targets for preterm labour. PLoS One 8, e56946.
Hannan, N.J., Jones, R.L., White, C.A., Salamonsen, L.A., 2006. The chemokines, CX3CL1, CCL14, and CCL4, promote human trophoblast migration at the feto-maternal interface. Biol. Reprod. 74, 896–904.
Harnett, E.L., Dickinson, M.A., Smith, G.N., 2007. Dose-dependent lipopolysaccharide-induced fetal brain injury in the guinea pig. Am. J. Obstet. Gynecol. 197 (179), e171–e177.
Hetz, C., 2012. The unfolded protein response: controlling cell fate decisions under ER stress and beyond. Nat. Rev. Mol. Cell Biol. 13, 89–102.
Iwawaki, T., Akai, R., Yamanaka, S., Kohno, K., 2009. Function of IRE1 alpha in the placenta is essential for placental development and embryonic viability. Proc. Natl. Acad. Sci. USA 106, 16657–16662.
Jabbour, H.N., Boddy, S.C., 2003. Prostaglandin E2 induces proliferation of glandular epithelial cells of the human endometrium via extracellular regulated kinase 1/2-mediated pathway. J. Clin. Endocrinol. Metab. 88, 4481–4487.
Jaeger, L.A., Spiegel, A.K., Ing, N.H., Johnson, G.A., Bazer, F.W., Burghardt, R.C., 2005. Functional effects of transforming growth factor beta on adhesive properties of porcine trophectoderm. Endocrinology 146, 3933–3942.
Jeong, W., Bae, H., Lim, W., Bazer, F.W., Song, G., 2017. Differential expression and functional roles of chemokine (C-C motif) ligand 23 and its receptor chemokine (C-C motif) receptor type 1 in the uterine endometrium during early pregnancy in pigs. Dev. Comp. Immunol. 76, 316–325.
Jeong, W., Jung, S., Bazer, F.W., Song, G., Kim, J., 2016. Epidermal growth factor: porcine uterine luminal epithelial cell migratory signal during the peri-implantation period of pregnancy. Mol. Cell. Endocrinol. 420, 66–74.
Jeong, W., Kim, J., Bazer, F.W., Song, G., 2014. Stimulatory effect of vascular endothelial growth factor on proliferation and migration of porcine trophectoderm cells and their regulation by the phosphatidylinositol-3-kinase-AKT and mitogen-activated protein kinase cell signaling pathways. Biol. Reprod. 90, 50.
Kearse, M., Moir, R., Wilson, A., Stones-Havas, S., Cheung, M., Sturrock, S., Buxton, S., Cooper, A., Markowitz, S., Duran, C., Thierer, T., Ashton, B., Meintjes, P., Drummond, A., 2012. Geneious Basic: an integrated and extendable desktop software platform for the organization and analysis of sequence data. Bioinformatics 28, 1647–1649.
Kitaya, K., Nakayama, T., Okubo, T., Kuroboshi, H., Fushiki, S., Honjo, H., 2003. Expression of macrophage inflammatory protein-1beta in human endometrium: its role in endometrial recruitment of natural killer cells. J. Clin. Endocrinol. Metab. 88, 1809–1814.
Lim, W., Bae, H., Bazer, F.W., Song, G., 2017a. Stimulatory effects of fibroblast growth factor 2 on proliferation and migration of uterine luminal epithelial cells during early pregnancy. Biol. Reprod. 96, 185–198.
Lim, W., Bae, H., Bazer, F.W., Song, G., 2018. Cell-specific expression and signal transduction of C-C motif chemokine ligand 2 and atypical chemokine receptors in the porcine endometrium during early pregnancy. Dev. Comp. Immunol. 81, 312–323.
Lim, W., Choi, M.J., Bae, H., Bazer, F.W., Song, G., 2017b. A critical role for adiponectin-mediated development of endometrial luminal epithelial cells during the peri-implantation period of pregnancy. J. Cell Physiol. 232, 3146–3157.
Liong, S., Lappas, M., 2014. Endoplasmic reticulum stress is increased after spontaneous labor in human fetal membranes and myometrium where it regulates the expression of prolabor mediators. Biol. Reprod. 91, 70.
Liu, A.X., He, W.H., Yin, L.J., Lv, P.P., Zhang, Y., Sheng, J.Z., Leung, P.C., Huang, H.F., 2011. Sustained endoplasmic reticulum stress as a cofactor of oxidative stress in decidual cells from patients with early pregnancy loss. J. Clin. Endocrinol. Metab. 96, E493–E497.
Mathew, D.J., Lucy, M.C., R, D.G., 2016. Interleukins, interferons, and establishment of pregnancy in pigs. Reproduction 151, R111–R122.
Menten, P., Wuyts, A., Van Damme, J., 2002. Macrophage inflammatory protein-1. Cytokine Growth Factor Rev. 13, 455–481.
Mulayim, N., Palter, S.F., Kayisli, U.A., Senturk, L., Arici, A., 2003. Chemokine receptor expression in human endometrium. Biol. Reprod. 68, 1491–1495.
Ramhorst, R., Grasso, E., Paparini, D., Hauk, V., Gallino, L., Calo, G., Vota, D., Perez Leiros, C., 2016. Decoding the chemokine network that links leukocytes with decidual cells and the trophoblast during early implantation. Cell Adhes. Migr. 10, 197–207.
Red-Horse, K., Drake, P.M., Gunn, M.D., Fisher, S.J., 2001. Chemokine ligand and receptor expression in the pregnant uterus: reciprocal patterns in complementary

cell subsets suggest functional roles. Am. J. Pathol. 159, 2199–2213.
Spencer, T.E., Bazer, F.W., 2004. Conceptus signals for establishment and maintenance of pregnancy. Reprod. Biol. Endocrinol. 2, 49.
Tayade, C., Black, G.P., Fang, Y., Croy, B.A., 2006. Differential gene expression in endometrium, endometrial lymphocytes, and trophoblasts during successful and abortive embryo implantation. J. Immunol. 176, 148–156.
Wang, G., Johnson, G.A., Spencer, T.E., Bazer, F.W., 2000. Isolation, immortalization, and initial characterization of uterine cell lines: an in vitro model system for the porcine uterus. In Vitr. Cell. Dev. Biol. Anim. 36, 650–656.
Wessels, J.M., Linton, N.F., van den Heuvel, M.J., Cnossen, S.A., Edwards, A.K., Croy, B.A., Tayade, C., 2011. Expression of chemokine decoy receptors and their ligands at the porcine maternal-fetal interface. Immunol. Cell Biol. 89, 304–313.
Xu, D.X., Wang, H., Zhao, L., Ning, H., Chen, Y.H., Zhang, C., 2007. Effects of low-dose lipopolysaccharide (LPS) pretreatment on LPS-induced intra-uterine fetal death and preterm labor. Toxicology 234, 167–175.
Yung, H.W., Calabrese, S., Hynx, D., Hemmings, B.A., Cetin, I., Charnock-Jones, D.S., Burton, G.J., 2008. Evidence of placental translation inhibition and endoplasmic reticulum stress in the etiology of human intrauterine growth restriction. Am. J. Pathol. 173, 451–462.
Zhao, M., Chen, Y.H., Chen, X., Dong, X.T., Zhou, J., Wang, H., Wu, S.X., Zhang, C., Xu, D.X., 2014. Folic acid supplementation during pregnancy protects against lipopolysaccharide-induced neural tube defects in mice. Toxicol. Lett. 224, 201–208.
Zlotnik, A., Yoshie, O., 2012. The chemokine superfamily revisited. Immunity 36, 705–716.